30% Reach Increase via Low-complexity Hybrid HD/SD FEC and Improved 4D Modulation

30% Reach Increase via Low-complexity Hybrid HD/SD FEC and Improved 4D Modulation

Gabriele Liga, *Member, IEEE,* Bin Chen, *Member, IEEE,* Sjoerd van der Heide, *Student Member, IEEE,* Alireza Sheikh, *Member, IEEE,* Menno van den Hout, Chigo Okonkwo, *Senior Member, IEEE,* and Alex Alvarado, *Senior Member, IEEE*

***Abstract*—Current optical coherent transponders technology is driving data rates towards 1 Tb/s/λ and beyond. This trend requires both high-performance coded modulation schemes and efficient implementation of the forward-error-correction (FEC) decoder. A possible solution to this problem is combining advanced multidimensional modulation formats with low-complexity *hybrid* HD/SD FEC decoders. Following this rationale, in this paper we combine two recently introduced coded modulation techniques: the geometrically-shaped 4D-64 polarization ring-switched and the soft-aided bit-marking-scaled reliability decoder. This joint scheme enabled us to experimentally demonstrate the transmission of 11$\times$218 Gbit/s channels over transatlantic distances at 5.2 bit/4D-sym. Furthermore, a 30% reach increase is demonstrated over PM-8QAM and conventional HD-FEC decoding for product codes.**

I. Introduction

Commercially available optical line rates have today reached 800 Gbit/s/λ, and they are rapidly heading towards 1 Tbit/s/λ and beyond, thus exerting unprecedented pressure on the optical transponder electronics. Such high data rates require high-performance yet implementation-efficient coded modulation schemes. Whilst high spectral-efficiency transmission can be provided by cleverly designed high-order modulation formats, low-complexity forward error correction (FEC) schemes are key to keep manageable power consumption in next-generation high-speed optical line cards.

Although soft-decision (SD)-FEC decoding represents the current gold-standard for FEC decoders in long-haul coherent optical communications, it entails high decoding complexity and dataflow, which makes its adoption into next-generation high-throughput line cards challenging [1]. Therefore, solutions which trade-off performance for a lower decoding complexity are becoming increasingly attractive [2]. Along the path traced by Chase in 1972 [3], hybrid hard-decision (HD)/SD decoders have been recently reproposed in optical communications as a low-complexity alternative to fully-fledged SD-FEC schemes [4]–[7]. In these schemes, reliability metrics are used to assist a standard HD decoder to improve its performance, whilst keeping the complexity of the overall decoder of the same order as that of algebraic HD decoding. These new decoding algorithms have been applied to both product codes (PCs) and staircase codes, showing substantial coding gains (0.2–0.8 dB) compared to its traditional HD counterpart, referred to as iterative bounded distance decoder (iBDD) [8, Sec. II-A]. One such decoding algorithm is the soft-aided bit marking (SABM) algorithm which was introduced in [9] and later extended in [7] to incorporate so-called scaled reliabilities (SRs), defined in [5], in the decoding process. This variant of SABM, named SABM-SR, was shown to outperform iBDD and SABM by up to 0.8 dB and 0.3 dB, respectively, with only minor additional complexity [7]. From a complexity/performance trade-off perspective, other attractive coding schemes have been recently proposed, e.g. in [10], [11].

In combination with FEC, constellation shaping has been demonstrated to be a viable solution for providing additional signal-to-noise ratio (SNR) gains at a given spectral efficiency (SE). In particular, geometrical shaping can be easily coupled with FEC and only requires straightforward modifications of the mapper and demapper. Recently, the four-dimensional 64-ary polarization-ring-switching (4D-64PRS) format, introduced in [12], was demonstrated to outperform other notable 4D modulation formats (see e.g., [13]) at a nominal SE of 6 bit/4D-sym [12], [14], thus representing a viable solution for long-reach 400G (dual-carrier) transponders.

In this work, we combine the low-complexity SABM-SR decoder and a PC-coded 4D-64PRS modulation format, enabling transmission of 11$\times$218 Gbit/s over transatlantic distances ($\geq$ 5,000 km) at 5.2 bit/symbol. Moreover, we demonstrate a total 30% reach increase over polarization multiplexed 8-quadrature amplitude modulation (PM-8QAM) and iBDD decoding.

II. Coded modulation with PC-coded 4D-64PRS and SABM-SR algorithm

A PC code array (see Fig. 1a) consists of a $n \times n$ matrix where both rows and columns are allowed codewords in in a so-called *component code* codebook. PCs are high performance HD codes thanks to the iBDD procedure. As illustrated in 1a, such a procedure consists in iteratively decoding the received PC array using the algebraic BDD algorithm on the component code, first by rows and then by columns. The main limitations of the iBDD are *failures* and *miscorrections*. When

G. Liga, A. Sheikh, and A. Alvarado are with the Signal Processing Systems (SPS) Group, Department of Electrical Engineering, Eindhoven University of Technology, The Netherlands. S. van der Heide, M. van den Hout and C. Okonkwo are with the Electro-Optical Communications (ECO) Group, Department of Electrical Engineering, Eindhoven University of Technology, The Netherlands e-mail: g.liga@tue.nl.

B. Chen is with the School of Computer Science and Information Engineering, Hefei University of Technology, China, and the Signal Processing Systems (SPS) Group, Department of Electrical Engineering, Eindhoven University of Technology, The Netherlands.

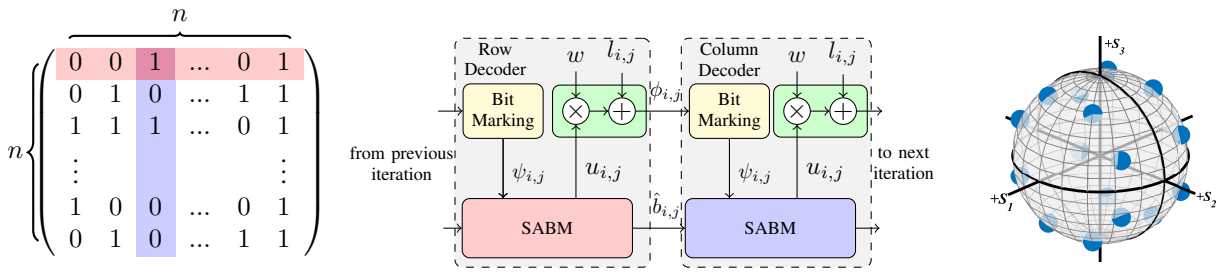

(a) (b) (c)

Fig. 1: Illustration of a square PC array a. Schematic diagram of one iteration of the SABM-SR algorithm b, and representation of the 4D-64PRS modulation format on the Poincaré sphere c.

the BDD finds an allowed codeword differing by up to t bits from the received one, where t is the error correction capability of the code, it declares a successful decoding. A failure occurs when the received codeword and any possible transmitted codeword differ by a number of bits greater than t. Finally, when a codeword is found within t bit positions but it does not correspond to the transmitted one, a miscorrection occurs. Note how a miscorrection is still detected by the BDD as a successful decoding.

The idea of the SABM algorithm is to minimize both failures and miscorrections via *bit marking* and *bit flipping*. The bit marking is performed via a bitwise reliability measure on the received bits, such as the log-likelihood ratio (LLR). The marking process consists in assigning each bit to one of following two classes: (i) highly-reliable bits (HRBs), (ii) highly-unreliable bits (HUBs). This is done by setting an optimal threshold on the magnitude of the LLR. The HRB class is used to prevent miscorrections arising from the iBDD as the core HD decoder for product-like codes: whenever the BDD attempts to flip an input bit which is flagged as a HRB a miscorrection is detected. Failures are instead avoided by performing another decoding attempt after the least reliable bit of the incoming binary vector is flipped. A more comprehensive description of the SABM algorithm can be found in [4].

The SABM-SR algorithm extends SABM by updating the bit reliability using the iterative HD decoding [7]. This is performed via SRs, which are a heuristic reliability metric proposed in [5], and obtained by linearly combining the scaled BDD hard output bits with the channel reliability. The workflow of one iteration of the SABM-SR algorithm is illustrated in Fig. 1b for PCs. For each output bit $\hat{b}_{i,j}$ in row i and column j of the core BDD, the SABM decoder computes quantized information $u_{i,j}$ based on the decoding state information of the BDD itself. In particular, $u_{i,j}$ is set to -1 and $+1$ to successfully decoded bits 0 and 1, respectively. When a failure occurs $u_{i,j}$ is instead set to 0. The SRs $\phi_{i,j}$ are calculated at each iteration for both row and column decoding, namely, $\phi_{i,j} = w u_{i,j} + l_{i,j}$, where $l_{i,j}$ are the channel LLRs and w are optimized weights through density evolution [5] for row/column decoding. Based on the updated SRs, a new bit marking is performed and a new mask of HUBs $\psi_{i,j}$ is passed to the SABM column decoder which then repeats the process.

In this paper, SABM-SR is used in combination with the recently introduced 4D-64PRS modulation format operating at a nominal SE of 6 bit/sym (64 points in 4D) [12]. The 4D-64PRS is obtained via a joint optimization of both constellation coordinates and binary labeling to maximize the generalized mutual information (GMI) in a nonlinear optical fiber channel. The resulting constellation is constant modulus in 4D and its representation in the Poincaré sphere is illustrated in Fig. 1c. Although the 4D-64PRS is specifically designed (via the GMI) to minimize post SD-FEC bit error rate (BER), because of the high rate of operation and its geometrical regularity, similar performance improvements are also expected with hybrid HD/SD decoders such as the SABM-SR. Moreover, for pure HD decoders pre-FEC BER is a strong performance predictor. Thus, 4D-64PRS is a convenient choice due to its improved pre-FEC BER performance compared to other more conventional 6 bit/4D symbol formats such as PM-(star)-8QAM (as shown in Sec. III).

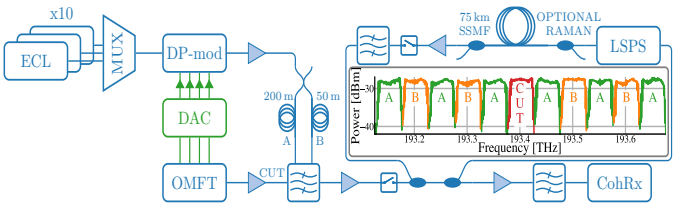

Fig. 2: Schematic diagram of the experimental testbed. On the right-hand side the received spectrum after $N = 80$ circulations (6,000 km) of EDFA-only amplification. The CUT is depicted in the center position but is tested in all 11 positions in the experiment.

III. Transmission Performance

The experimental testbed used for transmission is illustrated in Fig. 2. Uncoded sequences of 2^{16} symbols are generated offline, filtered by a root-raised-cosine with 1% roll-off at 41.79 GBd, pre-compensated for transmitter impairments, and uploaded to a 100-GSa/s digital-to-analog converter (DAC). The channel under test (CUT), chosen among any of the 11 tested C-band channels, is modulated by the optical-multi-format transmitter (OMFT), consisting of an external cavity laser (ECL), a dual-polarization optical modulator (DP-mod), and RF driving circuits, and subsequently amplified. The loading channels are generated using the multiplexed output of 10 ECLs and the DP-mod. The channels are then amplified, split into even and odd, decorrelated by 10,200 (50 m) and 40,800 symbols (200 m) respectively, and finally multiplexed together with the CUT on a 50-GHz grid using a multi-port optical tunable filter (OTF). The resulting signal

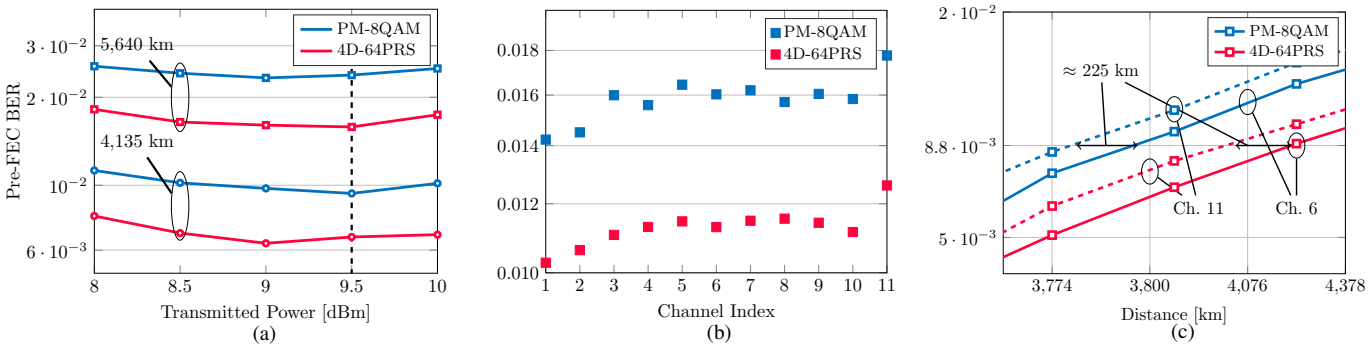

Fig. 3: Experimental results. Pre-FEC BER vs total transmitted power for ch. 6 at $N = 55$ and $N = 75$ a. Pre-FEC BER vs. channel index at 9.5 dBm total transmitted power and after $N = 55$ circulations b. Pre-FEC BER vs. transmission distance for ch. 6 at 9.5 dBm total transmitted power c.

is transmitted over the recirculating loop, which consists of a loop-synchronous polarization scrambler (LSPS), a 75-km span of standard single-mode fiber (SSMF), an erbium-doped fiber amplifier (EDFA), an acousto-optical modulator, and an OTF used for gain flattening. Fig. 2 (right) shows the optical spectrum after $N = 80$ circulations, corresponding to a 6,000 km transmission. The optical signal exiting the loop is then optically amplified, filtered by a wavelength-selective switch, and digitized by a conventional intradyne coherent receiver. Offline digital signal processing includes front-end correction, frequency-offset compensation, chromatic dispersion compensation, and multiple-input multiple-output equalization with in-loop blind phase search.

To select the optimum transmitted power, a pre-FEC BER characterization was first performed. Two modulation formats were compared: Gray-labelled PM-(star)-8QAM and 4D-64PRS. Fig. 3a shows the pre-FEC BER vs. total transmitted power for the central of the 11 transmitted channels (ch. 6) after 4,135 km and 5,640 km ($N = 55$ and 75, respectively). As the BER is essentially constant in the power range 8.5-9.5 dBm regardless of the distance and modulation format, a transmitted power of 9.5 dBm was selected as near-optimal for all distances and modulation formats investigated. Fig. 3b shows the pre-FEC BER for the 11 transmitted channels over a distance of 4,135 km ($N = 55$) and both modulation formats here investigated. The pre-FEC BER only exhibits minor fluctuations across the transmitted channels with ch. 11 being the worst-performing channel. However, for the purpose of demonstrating the SABM-SR gains and for experimental convenience, only the central channel (ch. 6) was used for evaluating the performance of the coded system. As shown in Fig. 3c, using ch. 11 as opposed to ch. 6 would result in a (pre-FEC) transmission distance penalty of about 225 km for both PM-8QAM, and 4D-64PRS modulation formats. Coding gains are, however, expected to be preserved for all transmitted channels.

For the evaluation of the coded transmission performance, the uncoded transmitted bits in the experimental traces were interleaved and scrambled to match the required number of randomly transmitted codewords. A PC using a 1-bit extended Bose-Chaudhuri-Hocquenghem (BCH) component code with information length, block length, and code rate of 239 and 256, and 0.87, respectively is considered, resulting in a net SE of 5.2 bit/4D-sym. As discussed in [4], the SABM-SR algorithm requires both the optimization of the number of iterations m over which miscorrection detection is performed and of the vector of weights $\boldsymbol{w} = [w_1, w_2, ..., w_m]$, where w_i represents the weight utilized at decoding iteration i for both row and column decoding (see Fig. 1a). After numerical optimization, we found that $m = 5$ and $\boldsymbol{w} = [3.42, 3.87, 4.08, 4.27, 4.49]$ are optimal values when a PC with extended BCH (256, 239) as a component code is used.

Fig. 4 shows the post-FEC BER vs. transmission reach for PM-8QAM and 4D-64PRS. When iBDD was used (diamond markers), the 4D-64PRS (red curves) showed a 12.5% reach increase at a post-FEC BER of 10^{-7} compared to PM-8QAM (blue curves). As expected, this gain is the same as the pre-FEC BER gain achieved by 4D-64PRS at BER=$8.8 \cdot 10^{-3}$ (inset), corresponding to a post-FEC BER of 10^{-7} for iBDD. The SABM decoder (square markers) yielded a 10.5% reach increase when used with either 4D-64PRS or with PM-8QAM. Furthermore, SABM-SR achieved a 16.5% reach increase compared to iBDD, regardless of the modulation format used. Thus, using SABM-SR led to an additional 6% reach increase compared to SABM. Combining SABM-SR and 4D-64PRS (red curve, circle markers) yielded a remarkable 30% reach increase vs. PM-8QAM with iBDD. Finally, Fig. 4 shows that transatlantic transmission ($\geq$ 5,000 km) was achieved using PC-coded 4D-64PRS and SABM-SR at a net SE of 5.2 bit/4D-sym (for BER$\leq 10^{-7}$).

IV. Comparison with other PC decoders

In this section, the performance of SABM-SR is compared with two relevant baseline decoders: *miscorrection-free* iBDD (MF-iBDD) and SD turbo-product decoding (TPD) based on the Chase-Pyndiah algorithm [15]. MF-iBDD represents a lower-bound on the performance of iBDD, and is obtained preventing all miscorrection events via a genie-aided approach. TPD is instead a *fully-fledged* SD algorithm for PCs with near-optimal decoding performance [15].

Post-FEC BER performance vs. transmission distance is shown in Fig. 5. The SABM-SR decoder (circle markers) leads to a transmission reach extension of about 8% compared to MF-iBDD (dash-dotted lines) in both the case of a PM-8QAM and 4D-64PRS transmission. We remark that such an extension is due to a twofold advantage of SABM-SR over MF-iBDD:

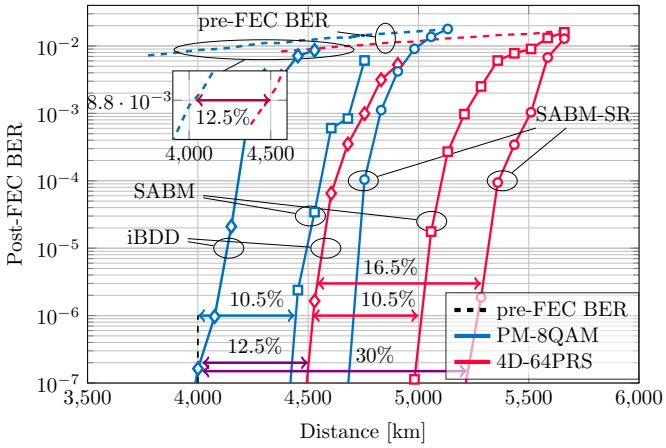

Fig. 4: Performance of SABM (squares) and SABM-SR (circles) compared to a conventional iBDD decoder (diamonds) using both PM-8QAM and 4D-64PRS modulation formats. Arrows indicate gains at a post-FEC BER of 10^{-7}.

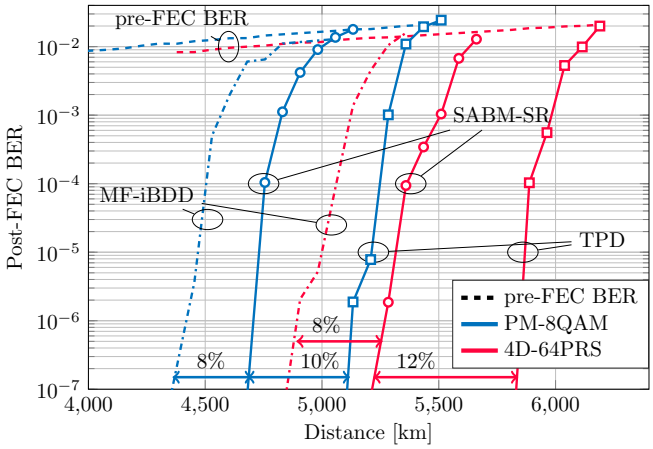

Fig. 5: Performance of SABM-SR (circles) compared to MF-iBDD (dash-dotted lines) and TPD (squares) with both PM-8QAM and 4D-64PRS modulation formats. Arrows indicate gains at a post-FEC BER of 10^{-7}.

i) the mitigation of decoding failures, which effectively extends the correction capability of the PC component code; ii) the *miscorrection recovery* which consists in detecting a miscorrection and in some cases also correctly recovering the codeword. TPD significantly outperforms SABM-SR (square markers in Fig. 5), thanks to the full processing of the SD information. This enables an additional 12% reach extension when 4D-64PRS is used. Similar coding gains (8% and 10% for MF-iBDD and TPD, respectively) are also observed for PM-8QAM. Although a detailed complexity analysis for SABM-SR is beyond the scope of this work, we note that: i) the gain of SABM-SR over MF-iBDD comes at expense of additional complexity (assuming MF-iBDD performance is approached using, e.g., anchor decoding [16]) due to the increased use of the BBD (for failures and miscorrections) and the SR updating; ii) TPD can be reasonably assumed to be within 1 and 2 orders of magnitude more complex than SABM-SR [4, Sec. IV-C] or other recently proposed reliability-based iBDD algorithms [6].

V. Conclusions

By combining an improved 4D modulation format (4D-64PRS) and the SABM-SR decoding algorithm, we transmitted 11×218 Gbit/s channels over a transatlantic distance at a net SE of 5.2 bit/4D-sym. A 30% reach increase vs. a conventional PM-8QAM transmission and HD decoding was also demonstrated. The results in this work highlight the potential of SABM-SR as a solution for low-power consumption/low-latency transceivers for long-haul dual-carrier 400G systems.

Acknowledgements

The work of G. Liga is funded by the EUROTECH programme (Marie Skodowska-Curie grant agreement No 754462). The work of G. Liga, A. Sheikh and A. Alvarado has received funding from the European Research Council (ERC) under the European Union's Horizon 2020 research and innovation programme (grant agreement No 757791). The work of A. Alvarado is supported by the Netherlands Organisation for Scientific Research (NWO) via the VIDI Grant ICONIC (project number 15685). The work of B. Chen is partially supported by the National Natural Science Foundation of China (NSFC) (grant 61701155). Partial funding from the NWO Gravitation Research Center for Integrated Nanophotonics (GA 024.002.033) is acknowledged.

References

[1] B. P. Smith, A. Farhood, A. Hunt, F. R. Kschischang, and J. Lodge, "Staircase codes: FEC for 100 Gb/s OTN," *J. Lightw. Technol.*, vol. 30, no. 1, pp. 110–117, Jan. 2012.

[2] Optical Internetworking Forum (OIF), "Technology options for 400G implementations," Jul. 2015.

[3] D. Chase, "A class of algorithms for decoding block codes with channel measurement information," *IEEE Trans. Inf. Theory*, vol. 18, no. 1, pp. 170–182, Jan. 1972.

[4] Y. Lei, B. Chen, G. Liga, X. Deng, Z. Cao, J. Li, K. Xu, and A. Alvarado, "Improved decoding of staircase codes: the soft-aided bit-marking (SABM) algorithm," *IEEE Trans. Commun.*, no. 12, pp. 8220–8232, Dec. 2019.

[5] A. Sheikh, A. Graell i Amat, and G. Liva, "Binary message passing decoding of product-like codes," *IEEE Trans. Commun.*, vol. 67, no. 12, pp. 8167–8178, Dec. 2019.

[6] C. Fougstedt, A. Sheikh, A. Graell i Amat, G. Liva, and P. Larsson-Edefors, "Energy-efficient soft-assisted product decoders," in *Proc. Optical Fiber Communication Conf. (OFC)*, San Diego, CA, 2019.

[7] G. Liga, A. Sheikh, and A. Alvarado, "A novel soft-aided bit-marking decoder for product codes," in *Proc. European Conf. Optical Communication (ECOC)*, Dublin, Ireland, Sep. 2019.

[8] A. Sheikh, A. Graell i Amat, and G. Liva, "On low-complexity decoding of product codes for high-throughput fiber-optic systems," in *Proc. IEEE Int. Symp. Turbo Codes & Iterative Information Processing (ISTC)*, Hong Kong, Hong Kong, Dec. 2018.

[9] Y. Lei, A. Alvarado, B. Chen, X. Deng, Z. Cao, J. Li, and K. Xu, "Decoding staircase codes with marked bits," in *Proc. IEEE 10th International Symposium on Turbo Codes & Iterative Information Processing (ISTC)*, Hong Kong, Hong Kong, Dec. 2018.

[10] M. Barakatain and F. R. Kschischang, "Low-Complexity Concatenated LDPC-Staircase Codes," *J. Lightw. Technol.*, vol. 36, no. 12, pp. 2443–2449, 2018.

[11] F. Steiner, E. Ben Yacoub, B. Matuz, G. Liva, and A. Graell i Amat, "One and Two Bit Message Passing for SC-LDPC Codes with Higher-Order Modulation," *Journal of Lightwave Technology*, vol. 37, no. 23, pp. 5914–5925, 2019.

[12] B. Chen, C. Okonkwo, H. Hafermann, and A. Alvarado, "Polarization-ring-switching for nonlinearity-tolerant geometrically-shaped four-dimensional formats maximizing generalized mutual information," *J. Lightw. Technol.*, vol. 37, pp. 3579–3591, Jul. 2019.

[13] K. Kojima, T. Yoshida, T. Koike-Akino, D. S. Millar, K. Parsons, M. Pajovic, and V. Arlunno, "Nonlinearity-tolerant four-dimensional 2A8PSK family for 5-7 bits/symbol spectral efficiency," *J. Lightw. Technol.*, vol. 35, no. 8, pp. 1383–1391, Apr. 2017.

[14] S. van der Heide, B. Chen, M. van den Hout, G. Liga, T. Koonen, H. Hafermann, A. Alvarado, and C. Okonkwo, "11,700 km transmission at 4.8 bit/4D-sym via four-dimensional geometrically-shaped polarization-ring-switching modulation," in *24th OptoElectronics and Communications Conference (OECC)*, Fukuoka, Japan, Jul. 2019.

[15] R. M. Pyndiah, "Near-optimum decoding of product codes: block turbo codes," *IEEE Trans. Commun.*, vol. 46, no. 8, pp. 1003–1010, Aug. 1998.

[16] C. Häger and H. D. Pfister, "Approaching miscorrection-free performance of product codes with anchor decoding," *IEEE Trans. Commun.*, vol. 66, no. 7, pp. 2797–2808, Mar. 2018.